*Article*

# Revisiting the Absorption Spectra of Polycyclic Aromatic Hydrocarbons over Porto (Portugal) by TD-DFT Calculations

**Guilherme M. Fernandes [1], Francisco J. D. Macedo [1], Joaquim C. G. Esteves da Silva [1,2]**
**and Luís Pinto da Silva [1,2,*]**

[1] Chemistry Research Unit (CIQUP), Institute of Molecular Sciences (IMS), Department of Geosciences, Environment and Territorial Planning, Faculty of Sciences, University of Porto (FCUP), R. Campo Alegre s/n, 4169-007 Porto, Portugal

[2] LACOMEPHI, GreenUPorto, Department of Geosciences, Environment and Territorial Planning, Faculty of Sciences, University of Porto, R. Campo Alegre s/n, 4169-007 Porto, Portugal

[*] Correspondence: luis.silva@fc.up.pt

**Abstract:** Brown carbon is a type of strong light-absorbing carbonaceous aerosol associated with radiative forcing. Nevertheless, the difficulty in correlating the chemical composition of brown carbon with its light absorption properties impairs the proper elucidation of its role in radiative forcing. Here, we have used a time-dependent density functional theory (TD-DFT)-based procedure to revisit the "real-world" absorption spectra of polycyclic aromatic hydrocarbons (PAHs) over the city of Porto, in Portugal, while correcting the spectra for their quantity in $PM_{10}$ particulate matter. Our aim is to, by comparing these new results with those obtained previously regarding $PM_{2.5}$ data, evaluate the role of different groupings of particulate matter in the light absorption of brown carbon. The results indicate that irrespective of the absorption spectra corresponding to their $PM_{10}$ or $PM_{2.5}$ data, the studied PAHs should contribute to radiative forcing by light absorption at UVA and (sub)visible wavelengths. However, the identity of the individual PAH species that contribute the most for the considered wavelengths can be quite different. Thus, different groupings of particulate matter appear to provide distinct contributions to light absorption and radiative forcing over the same location, even when considering the same class of molecular compounds.

**Keywords:** brown carbon; polycyclic aromatic hydrocarbons; radiative forcing; absorption spectra; density functional theory; organic aerosols

## 1. Introduction

There has been a significant increase in attention regarding light-absorbing aerosols due to data indicating that they possess an important role in radiative forcing [1–4]. This type of aerosol is mainly composed by a carbonaceous fraction, including both black carbon (BC) and brown carbon (BrC) [2,5]. While BC is known to be an important absorber due to its strong light absorption, the properties and importance of BrC still need to be better explored.

The absorption of solar radiation by BrC in ultraviolet (UV) and (sub)visible wavelengths can account for ~20–40% of aerosol absorption at 350 nm and 27% at 404 nm, with light absorption at higher wavelengths (such as 536 nm) being negligible [6–8]. In fact, there is evidence that BrC can dominate light absorption by aerosols at some wavelengths and/or specific regions of the globe [9,10]. Moreover, while the mass absorption of BrC can be lower than that of BC, its sheer abundance in continental aerosols makes UV absorption by carbonaceous aerosols quite relevant [5]. Nevertheless, the contribution of BrC to the absorption of solar radiation is still downplayed by different climate models [10,11]. This could explain why there are differences between model predictions and real measurements [3,12].

Understanding the photophysics and photochemistry of BrC aerosols is essential for the accurate modeling of radiative forcing. However, quantitatively predicting the contribution of BrC aerosols to light absorption is not trivial [3,13]. BrC aerosols can also be generated in the atmosphere by different processes, such as oxidation and solar irradiation [11,14,15]. BrC aerosols are also composed of diverse types of compounds with different light-absorption properties: polycyclic aromatics, phenols, biopolymers, or humic-like substances [2,16,17]. Finally, both the concentration and composition of BrC can change significantly across emission locations and sources [3,13]. The assessment of their properties is also impaired by the fact that online light absorption measurements of BrC are complex and that offline results provide data that differ from online approaches [18].

Despite all of this, polycyclic aromatic hydrocarbons (PAHs) have been identified as ubiquitous compounds [19] and important chromophores in BrC [4,5,8,20], while being also one of the most recurrent environmental contaminants, and being classified as persistent environmental pollutants [21,22]. While PAHs can be emitted into the atmosphere through natural burning events, the main contribution comes from anthropogenic sources, such as motor vehicles, coal burning, and industrial activities [23].

Given this, the reliable determination of the atmospheric light-absorption spectra of PAHs is essential for a more complete understanding and prediction of the radiative forcing effect of BrC aerosols. To address this, our study aims to use a computational chemistry approach to model the "real-world" absorption spectra of atmospheric PAHs by considering their experimental atmospheric concentration and speciation. This approach will determine which are the most relevant regions in UV and visible spectra of PAHs while correlating their light absorption to individual PAH species.

The computational chemistry calculations will be based on a density functional theory (DFT) approach, which has been increasingly and successfully used in the field of environmental sciences [24–27]. In fact, DFT calculations present some advantages over experimental studies as they do not require a high number of steps, such is the case of chemical synthesis, separation/purification, and characterization. DFT can also be extended to account for the time-dependent (TD) nature of electromagnetic waves and used to model excited states [28]. DFT calculations are also the most widely used approach to model the structures, photophysics, and photochemistry of organic molecules, including BrC [29–32].

This approach has already been used with success in the study of the "real-world" absorption spectra of PAHs over the atmosphere of several cities in different countries (Portugal, Spain, Italy, Greece, South Korea, and China) [33–36]. Our analysis indicated that PAHs have more intense light absorption in the UVB/UVA region and a more moderate one in the blue region of the visible spectrum. PAHs such as fluoranthene, benzo[*a*]anthracene, dibenzo[*a,h*]anthracene, and coronene were identified as the main contributors to UV absorption, while PAHs such as benzoperylene, benzo[*a*]pyrene, and indenopyrene were identified as capable of visible light absorption.

Interestingly, among cities studied in Europe, that of Porto (Portugal) was identified as the most potentially affected by PAH-induced radiative forcing [34], making it a relevant place for understanding the role of PAHs and BrC aerosols. It should be noted that these studies regarding Porto were based on experimentally determined data of concentration and speciation of PAHs, obtained by collecting samples of $PM_{2.5}$ particulate at a traffic site between January 2013 and February 2014 [37]. Given this, there is the question of if the contribution of PAHs to light absorption over Porto is dependent or not on the type of particulate matter. Herein, in this study we revisit the TD-DFT study of the absorption spectra of PAHs over the city of Porto by using experimentally determined data obtained from collecting samples of $PM_{10}$ particulate matter (instead of $PM_{2.5}$) [38], while maintaining a similar period of sample collecting (May–June 2014). This type of study should help to clarify if PAHs present in different groupings of particulate matter have different contributions to the combined atmospheric absorption spectra over specific locations.

## 2. Computational Methods

A total of 19 PAHs were computed—naphthalene (NAP), acenaphthylene (ACY), acenaphthene (ACE), fluorene (FLO), phenanthrene (PHE), anthracene (ANT), fluoranthene (FLT), pyrene (PYR), *p*-terphenyl (pTP), retene (RET), benzo[*a*]anthracene (BaA), chrysene (CHR), benzo[*b*]fluoranthene (BbF), benzo[*k*]fluoranthene (BkF), benzo[*a*]pyrene (BaP), perylene (PER), indeno[1,2,3-*cd*]pyrene (InP), dibenzo[*a,h*]anthracene (DahA), and benzo[*g,h,i*]perylene (BghiP)—and then corrected with their experimental atmospheric levels over the city of Porto (Portugal), which were extracted from the work of Alves et al. [38]. These values correspond to those found in $PM_{10}$ road dust samples, which were obtained during a sampling campaign that took place between the 9 May and the 1 July 2014 at five main roads of the city of Porto [38]. More specifically, these samples were collected at five main roads in the city of Porto: Fernão Magalhães Avenue; Constituição Street; Boavista Avenue; Campo Alegre Street; and Campo Mártires da Pátria [38].

The present calculations were performed with the Gaussian 09 program package [39] at two different levels of theory. All calculations were made in the gas phase. First, the geometries of each PAH were optimized by using the PBE0 density functional [40] and the 6-31G(d,p) basis set, while vibrational calculations were made at the same level of theory to ensure that the obtained structures were minima in their potential energy surfaces. This functional was chosen because it usually provides accurate geometry optimizations of organic molecules [41–44].

The absorption properties (oscillator strengths and absorption wavelengths) were calculated by performing single-point vertical excitation calculations with a TD-DFT approach, by computing 10 singlet excited states on top of the structures obtained at the PBE0/6-31G(d,p) level of theory. These single-point calculations were performed with a 6-31+G(d,p) basis set and two different density functionals: BP86 and PBE0. BP86 is a generalized gradient approximation (GGA) functional composed of the Becke 1988 exchange functional and the Perdew 86 correlation functional [45]. BP86 was used previously in the study of the "real-world" absorption spectra of PAHs (and derivatives) over different locations of the globe, including Porto [34–36]. PBE0 is used here because in a previous study it was found that, while different density functionals present qualitatively identical results, the position of the peaks can undergo blue/red shifts depending on the employed functional [36]. So, to mitigate possible functional-dependent errors, we calculated the absorption spectra with two different functionals: PBE0 and BP86. In fact, it is widely known that there is not an overall "best-performing density functional", as distinct functionals can present different performances regarding the different class of molecules and electronic states under study [46–48].

The absorption spectrum for each PAH species was plotted with SpecDis software (version 1.71) [49] based on the 10 singlet excited state transitions calculated at the TD-DFT/6-31+G(d,p) level of theory. The curves were generated with a Gaussian band shape and a peak broadening of 0.16 eV. The combined theoretical absorption spectrum of all PAHs was obtained by adding the individual spectra, without considering the experimentally obtained concentrations, resulting in absorption intensities only composed of $\varepsilon$ ($mol^{-1}$ $cm^{-1}$) [49]. The next step was to correct the intensity values of the spectrum by considering the experimentally obtained concentrations of each PAH over Porto, which was achieved by multiplying the theoretical absorption intensity ($\varepsilon$) of each PAH by its measured amount over Porto (determined as $\mu g\, g^{-1}$ $PM_{10}$) [38]. This resulted in absorption intensities composed by absorption per amount ($\varepsilon \times \mu g\, g^{-1}$ $PM_{10}$). The global spectrum was then obtained as the sum of the individual spectra.

## 3. Discussion and Results

This study started with the analysis of the combined absorption spectra of the PAHs found over the city of Porto, within $PM_{10}$ particles, when calculated with the BP86 functional and corrected for their experimentally determined amount [38]. These amounts are the average quantities found for each PAH in the sampling campaign performed by

Alves et al. [38]. Using the same density functional (BP86) used in our previous evaluation of the absorption spectra of PAHs over Porto [34], in which $PM_{2.5}$ particulate-related data was used [37], should enable comparisons that help us to understand if there are relevant differences in terms of light absorption from chemical components of different particulate matter. The BP86-derived combined absorption spectrum can be found in Figure 1. It should be noted that both in Figures 1 and 2, absorption becomes zero below 200 nm. This should not be taken as an indication that the absorption of PAHs is really zero at those wavelengths, which is not the case. Those absorption intensities result simply from our choice of calculating 10 excited states for each molecule, which account for light absorption in the relevant UV–visible range.

This absorption spectrum (Figure 1) is characterized by stronger absorption in the UVB region, with the most intense peak with a maximum at ~287 nm. There are then two almost merged peaks, with identical intensity, at ~309 and ~323 nm. We can also observe two sharp peaks with moderate absorption in the UVC region (~217 and ~263 nm), as well as a relevantly weaker band (~240 nm). The absorption in the UVA region is characterized by the tail of the peak at ~323 nm and a weaker band at ~380 nm, while in the visible region there are two broader and somewhat moderate (in intensity) peaks at ~433 and ~482 nm.

There are some relevant differences regarding the BP86-derived absorption spectrum obtained previously by us for $PM_{2.5}$-derived PAHs over Porto [33,37]. One of them is that the spectrum obtained previously was only composed of four peaks (~240, ~280, ~330, and ~420 nm) and one tail (~470 nm) instead of the nine peaks of variable relative intensity observed in Figure 1. Furthermore, the more intense peak found before was present in the UVA region, instead of the UVB one. These differences can be attributed to the different chemical compositions and respective amounts of the groups of particulate matter. That is, for the $PM_{2.5}$ samples collected over Porto, 55 PAHs were identified and quantified [36]. As for the $PM_{10}$ samples, only 19 PAHs were detected [38]. Nevertheless, in general, some similarities can also be found, as both spectra (Figure 1 and in [34]) have more intense absorption in the UVB/UVA regions, followed by more moderate absorption in the UVC region and weaker absorption in the visible region. Thus, irrespective of possible differences in chemical composition, the absorption spectra associated with PAHs found in different groupings of particulate matter should present qualitatively similar shapes.
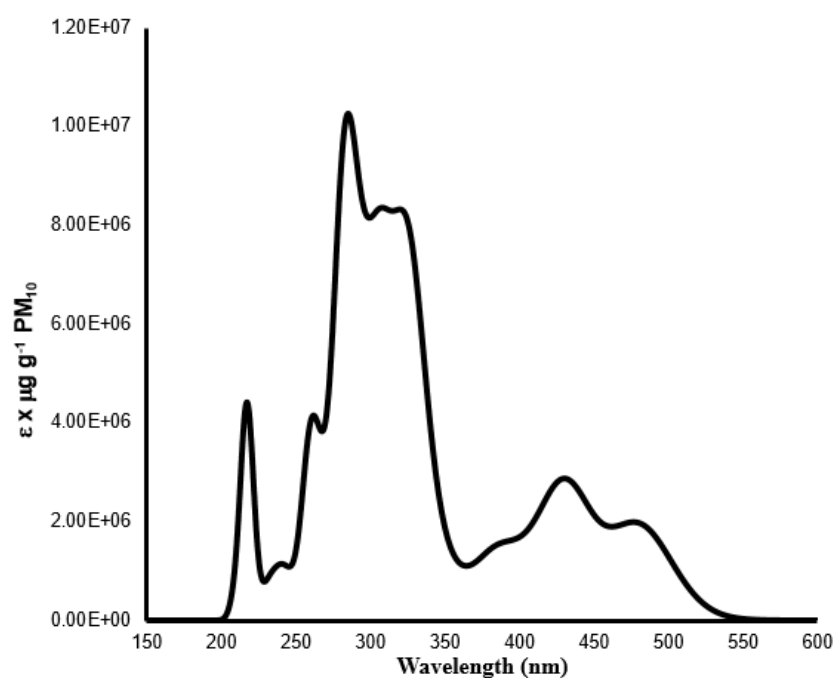


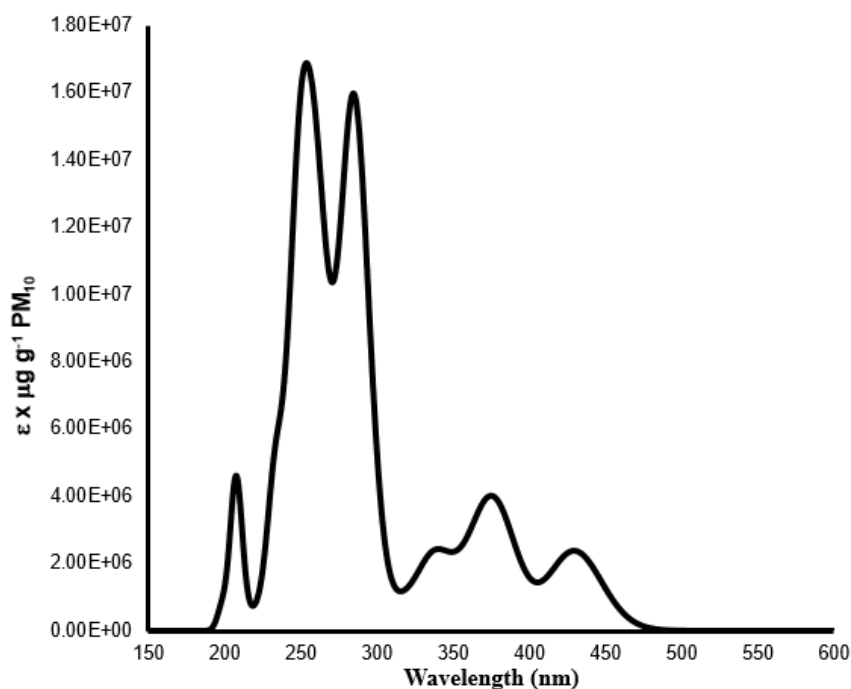**Figure 1.** Combined theoretical absorption spectra of PAHs, when corrected for their experimental mean amount ($\mu g\ g^{-1}\ PM_{10}$) [38] over Porto, by using TD-BP86/6-31+G(d,p).

**Figure 2.** Combined theoretical absorption spectra of PAHs, when corrected for their experimental mean amount ($\mu g\ g^{-1}\ PM_{10}$) [38] over Porto, by using TD-PBE0/6-31+G(d,p).

The combined absorption spectrum was also obtained at the TD-PBE0/6-31+G(d,p) level of theory and can be found in Figure 2. Quantitatively, this spectrum (Figure 2) is different from the one obtained at the TD-BP86/6-3+G(d,p) level of theory (Figure 1), as it is only composed of six peaks. However, qualitatively, the results are indeed quite similar, with the main difference being that the PBE0-related spectrum is blue-shifted when comparing with that obtained with the BP86 functional. That is, the stronger peak found in Figure 2 (~254 nm) corresponds to the stronger peak at ~287 nm in the BP86-derived spectrum (Figure 1). The second strongest peak in the PBE0-derived spectrum (~285 nm, Figure 2) can also be linked to the almost merged peaks at ~309/323 nm found in the BP86-based spectrum (Figure 1). The more moderate peak (~208 nm) in Figure 2 can also be correlated with that at ~217 nm and observed in Figure 1. Finally, the more moderate/weaker PBE0-based peaks found at ~337, ~377, and ~431 nm (Figure 2) appear to correspond to the BP86-related peaks found at ~380, ~433, and ~482 nm (Figure 1), respectively. Thus, and consistent with previous studies [35], the use of different density functionals result in absorption spectra with similar shape but quantitatively different results, with relevant blue-/red shifts in the position of the peaks, according to specific functionals.

After describing the atmospheric absorption spectra of PAHs over Porto, when derived from $PM_{10}$ particles, it should be noted that UVC radiation is completely filtered by the atmosphere. Furthermore, there is not expected much ground-level solar insolation at ~290–300 nm due to ozone absorption [50]. Thus, the absorption peaks that should contribute the most for PAH-related radiative forcing should be those with wavelengths higher than ~300 nm. For the PBE0-related spectrum (Figure 2), those peaks are those with wavelength maxima at ~337, ~377, and ~431 nm. For the BP86-based spectrum (Figure 1), those should be the ones with maxima at ~323, ~380, ~433, and ~482 nm. However, as we have attributed the ~323 nm peak to that at ~285 nm (in the PBE0-related spectrum), we have excluded it from further analysis. Thus, the $PM_{10}$-related PAHs, over Porto, should only contribute to radiative forcing by relatively moderate/weaker absorption at the UVA region and at short (sub)visible wavelengths. This is in line with reports that ~20–40% of aerosol absorption is at 350 nm and 27% at 404 nm, while absorption at higher wavelengths is not relevant [6–8]. Interestingly, the previous results obtained by us for the light absorption of $PM_{2.5}$-related PAHs over Porto (at the BP86 level of theory)

indicated that the most relevant absorption peaks for radiative forcing should have maxima at ~330 and ~420 nm (and an absorption tail at ~470 nm) [34]. These data are qualitatively in line with those obtained here with the same functional, indicating that overall, the combined absorption spectra of PAHs are similar, irrespective of the considered groupings of particulate matter.

Besides determining the absorption spectra, it is also of importance to determine the relative contribution of each individual absorption to the relevant absorption peaks. Thus, the next step of this study was then to decompose the absorption intensity of the bands referred above in the relative contribution of individual PAHs (Table 1). To better compare with the results previously obtained by us toward Porto [34], we performed this decomposition relative only to BP86-related results.

**Table 1.** Contribution (in %) of PAH molecules to the absorption intensity at different wavelengths (in nm) over Porto. Only molecules with contributions higher or equal than 5% are presented.

| PAH | ~380 nm | ~433 nm | ~482 nm |
|---|---|---|---|
| FLT | 5% | | |
| CHR | 8% | | |
| BbF | 63% | | |
| DahA | 5% | | |
| InP | 9% | | 7% |
| BkF | | 41% | |
| BaP | | 40% | |
| BghiP | | 10% | |
| PER | | | 89% |

Analysis of Table 1 indicates that the absorption peak at ~380 nm is explained in large part by BbF, followed (with large differences) by InP, CHR, and FLT/DahA. As for the peak at ~433 nm, it is explained mostly by identical contributions from BkF and BaP, and by smaller contributions from BghiP. Lastly, the absorption in the (sub)visible region is explained almost exclusively by PER, with some quite smaller contributions by InP.

Interestingly, relevant differences can be found between the results presented here (Table 1) and those found before for the same city but with $PM_{2.5}$-derived data [34]. That is, while in this study, absorption at ~433 nm (the peak with the most similar wavelength maxima between studies) is explained by BkF (41%), BaP (40%), and PER (10%), the absorption at ~420 nm was previously mainly explained by contributions from BghiP (32.8%), InP (20.6%), BaP (19.3%), benzo[*j*]fluoranthene (9.3%), and BkF (7.0%) [34]. Thus, only BaP and BkF are the same relevant contributors between the different studies and with quite different contribution magnitudes. By their turn, PER is only relevant at this wavelength when found in $PM_{10}$-based samples, while BghiP, InP, and benzo[*j*]fluoranthene are only important contributors when considering their $PM_{2.5}$-based concentration. Thus, this data demonstrates that the chemical components of different groupings of particulate matter can present relevant differences regarding light absorption over the same location, even if we compare the same molecular class. These differences, at least over the city of Porto, appear to be more related with individual contributions from PAH-based species, instead of being related with the general shape of the combined absorption spectra.

## 4. Conclusions

Herein, we have revisited the study of the "real-world" light absorption spectra of PAHs over the Portuguese city of Porto by using a TD-DFT-based computational chemistry approach with corrections from experimental studies regarding the chemical composition of $PM_{10}$ samples (which detected and quantified 19 PAH species). These results were

subsequently compared with those previously obtained for PAHs detected in PM$_{2.5}$ samples over the same city, in a similar period. With this approach, our goal was then to try to determine if the contribution of PAHs toward light absorption is dependent on their presence in different groupings of particulate matter.

Our results allowed the determination that PAH-induced radiative forcing over the city of Porto should be more limited to light absorption at both UVA and (sub)visible wavelengths. Moreover, BbF, BkF, BaP, and PER were found to be the most relevant contributors to the different absorption peaks of the combined absorption spectra. Thus, these PAHs should be targeted to address PAH-induced radiative forcing over Porto. Interestingly, while the general combined absorption spectra of PAHs detected in both PM$_{2.5}$ and PM$_{10}$ samples have similar shape, the contribution of individual species appear to be quite different. Thus, different groupings of particulate matter appear to provide distinct contributions to light absorption and radiative forcing over the same location, even when considering the same class of molecular compounds.

## References

1. Andreae, M.O.; Gelencsér, A. Black carbon or brown carbon? The nature of light-absorbing carbonaceous aerosols. *Atmos. Chem. Phys.* **2006**, *6*, 3131–3148. [CrossRef]
2. Lei, Y.; Shen, Z.; Wang, Q.; Zhang, T.; Cao, J.; Sun, J.; Wang, L.; Xu, H.; Tian, J.; Wu, J. Optical characteristics and source apportionment of brown carbon in winter PM2.5 over Yulin in Northern China. *Atmos. Res.* **2018**, *213*, 27–33. [CrossRef]
3. Lin, P.; Liu, J.; Shilling, J.E.; Kathmann, S.M.; Laskin, J.; Laskin, A. Molecular characterization of brown carbon (BrC) chromophores in secondary organic aerosol generated from photo-oxidation of toluene. *Phys. Chem. Chem. Phys.* **2015**, *17*, 23312–23325. [CrossRef] [PubMed]
4. Zhu, C.-S.; Li, L.-J.; Huang, H.; Dai, W.-T.; Lei, Y.-L.; Qu, Y.; Huang, R.-J.; Wang, Q.-Y.; Shen, Z.-X.; Cao, J.J. n-Alkanes and PAHs in the Southeastern Tibetan Plateau: Characteristics and Correlations with Brown Carbon Light Absorption. *J. Geophys. Res. Atmos.* **2020**, *125*, e2020JD032666. [CrossRef]
5. Huang, R.-J.; Yang, L.; Cao, J.; Chen, Y.; Chen, Q.; Li, Y.; Duan, J.; Zhu, C.; Dai, W.; Wang, K.; et al. Brown Carbon Aerosol in Urban Xi'an, Northwest China: The Composition and Light Absorption Properties. *Environ. Sci. Technol.* **2018**, *52*, 6825–6833. [CrossRef] [PubMed]
6. Lack, D.A.; Langridge, J.M.; Bahreini, R.; Cappa, C.D.; Middlebrook, A.M.; Schwarz, J.P. Brown carbon and internal mixing in biomass burning particles. *Proc. Natl. Acad. Sci. USA* **2012**, *109*, 14802–14807. [CrossRef] [PubMed]
7. Liu, J.; Bergin, M.; Guo, H.; King, L.; Kotra, N.; Edgerton, E.; Weber, R.J. Size-resolved measurements of brown carbon in water and methanol extracts and estimates of their contribution to ambient fine-particle light absorption. *Atmos. Chem. Phys.* **2013**, *13*, 12389–12404. [CrossRef]
8. Xu, J.; Cui, T.; Fowler, B.; Fankhauser, A.; Yang, K.; Surratt, J.D.; McNeill, V.F. Aerosol Brown Carbon from Dark Reactions of Syringol in Aqueous Aerosol Mimics. *ACS Earth Space Chem.* **2018**, *2*, 608–617. [CrossRef]
9. Lin, G.; Penner, J.E.; Flanner, M.G.; Sillman, S.; Xu, L.; Zhou, C. Radiative forcing of organic aerosol in the atmosphere and on snow: Effects of SOA and brown carbon. *J. Geophys. Res. Atmos.* **2014**, *119*, 7453–7476. [CrossRef]
10. Saleh, R.; Marks, M.; Heo, J.; Adams, P.J.; Donahue, N.M.; Robinson, A.L. Contribution of brown carbon and lensing to the direct radiative effect of carbonaceous aerosols from biomass and biofuel burning emissions. *J. Geophys. Res. Atmos.* **2015**, *120*, 10285–10296. [CrossRef]
11. Frka, S.; Šala, M.; Kroflič, A.; Huš, M.; Čusak, A.; Grgić, I. Quantum Chemical Calculations Resolved Identification of Methylnitrocatechols in Atmospheric Aerosols. *Environ. Sci. Technol.* **2016**, *50*, 5526–5535. [CrossRef] [PubMed]

12. Chung, C.E.; Ramanathan, V.; Decremer, D. Observationally constrained estimates of carbonaceous aerosol radiative forcing. *Proc. Natl. Acad. Sci. USA* **2012**, *109*, 11624–11629. [CrossRef] [PubMed]

13. Lin, P.; Aiona, P.K.; Li, Y.; Shiraiwa, M.; Laskin, J.; Nizkorodov, S.A.; Laskin, A. Molecular Characterization of Brown Carbon in Biomass Burning Aerosol Particles. *Environ. Sci. Technol.* **2016**, *50*, 11815–11824. [CrossRef] [PubMed]

14. De Haan, D.O.; Tapavicza, E.; Riva, M.; Cui, T.; Surratt, J.D.; Smith, A.C.; Jordan, M.-C.; Nilakantan, S.; Almodovar, M.; Stewart, T.N.; et al. Nitrogen-Containing, Light-Absorbing Oligomers Produced in Aerosol Particles Exposed to Methylglyoxal, Photolysis, and Cloud Cycling. *Environ. Sci. Technol.* **2018**, *52*, 4061–4071. [CrossRef]

15. Phillips, S.M.; Bellcross, A.D.; Smith, G.D. Light Absorption by Brown Carbon in the Southeastern United States is pH-dependent. *Environ. Sci. Technol.* **2017**, *51*, 6782–6790. [CrossRef]

16. Adler, G.; Wagner, N.L.; Lamb, K.D.; Manfred, K.; Schwarz, J.P.; Franchin, A.; Middlebrook, A.M.; Washenfelder, R.A.; Womack, C.C.; Yokelson, R.J.; et al. Evidence in biomass burning smoke for a light-absorbing aerosol with properties intermediate between brown and black carbon. *Aerosol Sci. Technol.* **2019**, *53*, 976–989. [CrossRef]

17. Cheng, Z.; Atwi, K.; Yu, Z.; Avery, A.; Fortner, E.C.; Williams, L.; Majluf, F.; Krechmer, J.E.; Lambe, A.T.; Saleh, R. Evolution of the light-absorption properties of combustion brown carbon aerosols following reaction with nitrate radicals. *Aerosol Sci. Technol.* **2020**, *54*, 849–863. [CrossRef]

18. Cheng, Z.; Atwi, K.; El Hajj, O.; Ijeli, I.; Al Fischer, D.; Smith, G.; Saleh, R. Discrepancies between brown carbon light-absorption properties retrieved from online and offline measurements. *Aerosol Sci. Technol.* **2020**, *55*, 92–103. [CrossRef]

19. D'Hendecourt, L.; Ehrenfreund, P. Spectroscopic properties of polycyclic aromatic hydrocarbons (PAHs) and astrophysical implications. *Adv. Space Res.* **1997**, *19*, 1023–1032. [CrossRef]

20. Cheng, Y.; He, K.; Engling, G.; Weber, R.; Liu, J.; Du, Z.; Dong, S. Brown and black carbon in Beijing aerosol: Implications for the effects of brown coating on light absorption by black carbon. *Sci. Total Environ.* **2017**, *599–600*, 1047–1055. [CrossRef]

21. van der Gon, H.D.; van het Bolscher, M.; Visschedijk, A.; Zandveld, P. Emissions of persistent organic pollutants and eight candidate POPs from UNECE–Europe in 2000, 2010 and 2020 and the emission reduction resulting from the implementation of the UNECE POP protocol. *Atmos. Environ.* **2007**, *41*, 9245–9261. [CrossRef]

22. Mari, M.; Harrison, R.M.; Schuhmacher, M.; Domingo, J.L.; Pongpiachan, S. Inferences over the sources and processes affecting polycyclic aromatic hydrocarbons in the atmosphere derived from measured data. *Sci. Total Environ.* **2010**, *408*, 2387–2393. [CrossRef] [PubMed]

23. Kim, B.M.; Lee, S.-B.; Kim, J.Y.; Kim, S.; Seo, J.; Bae, G.-N.; Lee, J.Y. A multivariate receptor modeling study of air-borne particulate PAHs: Regional contributions in a roadside environment. *Chemosphere* **2016**, *144*, 1270–1279. [CrossRef]

24. Fu, Z.; Wang, Y.; Chen, J.; Wang, Z.; Wang, X. How PBDEs Are Transformed into Dihydroxylated and Dioxin Metabolites Catalyzed by the Active Center of Cytochrome P450s: A DFT Study. *Environ. Sci. Technol.* **2016**, *50*, 8155–8163. [CrossRef] [PubMed]

25. Krzemińska, A.; Paneth, P. DFT Studies of $S_N2$ Dechlorination of Polychlorinated Biphenyls. *Environ. Sci. Technol.* **2016**, *50*, 6293–6298. [CrossRef] [PubMed]

26. da Silva, L.P. Theoretical Study of the Ring-Opening of Epoxides Catalyzed by Boronic Acids and Pyridinic Bases. *J. Phys. Chem. C* **2017**, *121*, 16300–16307. [CrossRef]

27. da Silva, L.P. Mechanistic study of the role of hydrogen bond donors in the two-component organocatalysis of the ring-opening reaction of epoxides. *Mol. Catal.* **2019**, *474*, 110425. [CrossRef]

28. Adamo, C.; Jacquemin, D. The calculations of excited-state properties with Time-Dependent Density Functional Theory. *Chem. Soc. Rev.* **2012**, *42*, 845–856. [CrossRef]

29. Chen, J.Y.; Rodriguez, E.; Jiang, H.; Chen, K.; Frie, A.L.; Zhang, H.; Bahreini, R.; Lin, Y.-H. Time-Dependent Density Functional Theory Investigation of the UV–Vis Spectra of Organonitrogen Chromophores in Brown Carbon. *ACS Earth Space Chem.* **2020**, *4*, 311–320. [CrossRef]

30. Hede, T.; Murugan, N.A.; Kongsted, J.; Leck, C.; Ågren, H. Simulations of Light Absorption of Carbon Particles in Nanoaerosol Clusters. *J. Phys. Chem. A* **2014**, *118*, 1879–1886. [CrossRef]

31. Magalhães, A.C.O.; Da Silva, J.C.G.E.; Da Silva, L.P. Density Functional Theory Calculation of the Absorption Properties of Brown Carbon Chromophores Generated by Catechol Heterogeneous Ozonolysis. *ACS Earth Space Chem.* **2017**, *1*, 353–360. [CrossRef]

32. Dolomatov, M.Y.; Shutkova, S.A.; Bakhtizin, R.Z.; Dolomatova, M.M.; Latypov, K.F.; Gilmanshina, K.A.; Badretdinov, B.R. Structure of Asphaltene Molecules and Nanoclusters Based on Them. *Pet. Chem.* **2020**, *60*, 16–21. [CrossRef]

33. Pinto da Silva, L.; Dias, T.B.; Esteves da Silva, J.C.G. Modelling the absorption spectra of polycyclic aromatic hydrocarbons over Seoul, South Korea. *Environ. Technol. Innov.* **2019**, *17*, 100536. [CrossRef]

34. Sousa, J.; Pinto da Silva, L. Modelling the absorption properties of polycyclic aromatic hydrocarbons and derivatives over three European cities by TD-DFT calculations. *Sci. Total Environ.* **2019**, *695*, 133881. [CrossRef] [PubMed]

35. González-Berdullas, P.; da Silva, L.P. TD-DFT Monitoring of the Absorption Spectra of Polycyclic Aromatic Hydrocarbons over the Basque Country, Spain. *Sustain. Chem.* **2021**, *2*, 599–609. [CrossRef]

36. González-Berdullas, P.; Cruz, C.N.; Bandowe, B.A.; da Silva, J.C.E.; da Silva, L.P. A time-dependent density functional theory investigation of the atmospheric absorption spectra of polycyclic aromatic hydrocarbons (PAHs) and their derivatives (Alkyl-PAHs, oxygenated-PAHs, and Nitrated-PAHs) over an urban area in China. *J. Environ. Chem. Eng.* **2022**, *10*, 108853. [CrossRef]

37. Alves, C.A.; Vicente, A.M.; Custódio, D.; Cerqueira, M.; Nunes, T.; Pio, C.; Lucarelli, F.; Calzolai, G.; Nava, S.; Diapouli, E.; et al. Polycyclic aromatic hydrocarbons and their derivatives (nitro-PAHs, oxygenated PAHs, and azaarenes) in PM 2.5 from Southern European cities. *Sci. Total. Environ.* **2017**, *595*, 494–504. [CrossRef]

38. Alves, C.; Evtyugina, M.; Vicente, A.; Vicente, E.; Nunes, T.; Silva, P.; Duarte, M.; Pio, C.; Amato, F.; Querol, X. Chemical profiling of PM10 from urban road dust. *Sci. Total Environ.* **2018**, *634*, 41–51. [CrossRef]

39. Frisch, M.J.; Trucks, G.W.; Schlegel, H.B.; Scuseria, G.E.; Robb, M.A.; Cheeseman, J.R.; Scalmani, G.; Barone, V.; Mennucci, B.; Petersson, G.A.; et al. *Gaussian 09, revision D.01*; Gaussian, Inc.: Wallingford, CT, USA, 2013.

40. Adamo, C.; Barone, V. Toward reliable density functional methods without adjustable parameters: The PBE0 model. *J. Chem. Phys.* **1999**, *110*, 6158–6170. [CrossRef]

41. Barone, V.; Cimino, P.; Crescenzi, O.; Pavone, M. Ab initio computation of spectroscopic parameters as a tool for the structural elucidation of organic systems. *J. Mol. Struct. Theochem.* **2007**, *811*, 323–335. [CrossRef]

42. Jacquemin, D.; Preat, J.; Perpète, E.A.; Adamo, C. Absorption spectra of recently synthesised organic dyes: A TD-DFT study. *Int. J. Quantum Chem.* **2010**, *110*, 2121–2129. [CrossRef]

43. Le Bahers, T.; Adamo, C.; Ciofini, I. Photophysical Properties of 8-Hydroxyquinoline-5-sulfonic Acid as a Function of the pH: A TD-DFT Investigation. *J. Phys. Chem. A* **2010**, *114*, 5932–5939. [CrossRef] [PubMed]

44. Pinto da Silva, L.; Esteves da Silva, J.C.G. Computational Investigation of the Effect of pH on the Color of Firefly Bioluminescence by DFT. *ChemPhysChem* **2011**, *12*, 951–960. [CrossRef]

45. Becke, A.D. Density-functional thermochemistry. III. The role of exact exchange. *J. Chem. Phys.* **1993**, *98*, 5648–5652. [CrossRef]

46. Gronowski, M.; Kołos, R. A DFT Study on the Excited Electronic States of Cyanopolyynes: Benchmarks and Applications. *Molecules* **2022**, *27*, 5829. [CrossRef] [PubMed]

47. Gronowski, M. TD-DFT benchmark: Excited states of atoms and atomic ions. *Comput. Theor. Chem.* **2017**, *1108*, 50–56. [CrossRef]

48. Shi, B.; Nachtigallová, D.; Aquino, A.J.A.; Machado, F.B.C.; Lischka, H. High-level theoretical benchmark investigations of the UV-vis absorption spectra of paradigmatic polycyclic aromatic hydrocarbons as models for graphene quantum dots. *J. Chem. Phys.* **2019**, *150*, 124302. [CrossRef]

49. Bruhn, T.; Schaumlöffel, A.; Hemberger, Y.; Bringmann, G. SpecDis: Quantifying the comparison of calculated and experimental electronic circular dichroism spectra. *Chirality* **2013**, *25*, 243–249. [CrossRef]

50. *ASTM.G173-03*; Standard Tables for Reference Solar Spectral Irradiances: Direct Normal and Hemispherical on 37° Tilted Surface. ASTM International: West Conshohocken, PA, USA, 2012.